electronics

MDPI

Article

Tracking Control of Quadrotor UAVs with Prescribed Performance and Prescribed-Time Convergence Under Arbitrary Initial Conditions

Tiantian Xiao [1,2], Jinlong Guo [3,4], Jintao Chen [2], Dawei Sun [1,*], Daochun Li [1] and Jinwu Xiang [1]

[1] School of Aeronautical Science and Engineering, Beihang University, Beijing 100191, China; zb2105114@buaa.edu.cn (T.X.); lidc4@buaa.edu.cn (D.L.); xiangjw@buaa.edu.cn (J.X.)
[2] Department of Fundamental Theory, Qiyuan Lab, Beijing 100084, China; chenjintao@qiyuanlab.com
[3] National Center of Excellence for Engineer Education, Northwestern Polytechnical University, Xi'an 710072, China; guojinlong@mail.nwpu.edu.cn
[4] Department of Unmanned System, The 208th Research Institute, Beijing 102202, China
* Correspondence: dwsun@buaa.edu.cn

Abstract

Quadrotor unmanned aerial vehicles demonstrate broad application prospects, yet existing research still lacks a comprehensive solution that simultaneously addresses efficiency, disturbance rejection, environmental adaptability, and precision in their control performance. To achieve prescribed-time convergence and prescribed tracking performance, this work proposes a composite control scheme that integrates prescribed-performance control, disturbance estimation, and terminal sliding-mode control. First, a prescribed-time adaptive composite disturbance observer is developed to estimate and compensate for system composite disturbances, and a stability analysis shows that the disturbance estimation error converges to a small neighborhood of the origin within a prescribed time. Second, the system is decomposed into position and attitude subsystems, enabling tailored hierarchical control-law design and analysis based on their distinct dynamics. For position control, a prescribed-performance control method is employed, incorporating a prescribed-time performance function that accommodates large initial deviations, thereby guaranteeing convergence of the position-tracking errors to a small neighborhood within a specified time. For attitude control, a prescribed-time terminal sliding-mode surface and corresponding control law are designed to eliminate singularities and ensure convergence of the attitude errors to a small neighborhood within a predetermined time. The stability of both subsystems is rigorously substantiated through theoretical analysis. Finally, comparative simulation results confirm the effectiveness and superiority of the proposed control strategy.

Keywords: prescribed time; prescribed performance; disturbance observation; sliding mode

Check for updates

Academic Editor: Luca Patanè

Received: 14 December 2025
Revised: 9 January 2026
Accepted: 13 January 2026
Published: 16 January 2026

Copyright: © 2026 by the authors. Licensee MDPI, Basel, Switzerland. This article is an open access article distributed under the terms and conditions of the Creative Commons Attribution (CC BY) license.

1. Introduction

Quadrotor unmanned aerial vehicles (QUAVs) have demonstrated significant application potential in various domains, including disaster rescue, package delivery, and military reconnaissance, owing to their exceptional maneuverability and vertical take-off and landing capabilities [1]. However, in complex real-world operational environments, QUAVs still face substantial challenges in control efficiency, disturbance rejection, environmental adaptability, and trajectory-tracking accuracy [2]. Conventional control approaches typically focus on enhancing individual performance aspects, such as precise tracking

control or disturbance-rejection-based tracking control [3]; yet, the multifaceted nature of control performance has not been comprehensively addressed from multiple perspectives in existing studies.

To handle the coupled nonlinear dynamics inherent in QUAV models, hierarchical control strategies have been widely adopted. He Ming et al. [4] underscores the importance of hierarchical control architectures, providing theoretical support for the position-loop-attitude-loop hierarchical design employed in this work. Raffo et al. [5] proposes a backstepping-based cascaded control framework; however, its performance is highly sensitive to initial conditions. Iltayed et al. [6] designs an adaptive sliding-mode hierarchical controller, but the resulting convergence time depends on initial states, and its disturbance attenuation capability remains limited. A critical deficiency common to existing methods is the significant degradation of convergence performance under large initial state deviations, which fails to meet the stringent timeliness requirements of certain application scenarios.

Recent developments in resilient UAV control have further emphasized the importance of disturbance rejection in real-world tracking scenarios. Cui et al. [7] investigates cooperative path planning for autonomous aerial vehicles in wildlife tracking applications, demonstrating that robust coordination mechanisms are essential for maintaining performance under communication constraints and environmental uncertainties. Xu et al. [8] proposed an adaptive finite-time attitude tracking control scheme for quadrotors that addresses actuator faults and external disturbances with guaranteed prescribed performance, highlighting the critical need for fault-tolerant mechanisms with transient performance guarantees. Liu et al. [9] developed secure formation control strategies for multi-agent cyber-physical systems under denial-of-service (DoS) attacks and component faults, showing that resilient control architectures become essential when system reliability is compromised by adversarial conditions. These recent works underscore that modern UAV applications demand control strategies that can simultaneously handle disturbances, guarantee transient performance, and maintain robustness under adverse conditions—motivations that directly align with the objectives of this paper.

To address the robust control problem of QUAVs, researchers have explored Prescribed-Time Control (PTC) methods that use time-varying gain functions to guarantee system convergence in a prescribed finite time. For instance, Polyakov et al. [10] establish a rigorous theoretical foundation for PTC, while Wang et al. [11] apply it to UAV control. Liu Hao et al. [12] design a prescribed-time sliding-mode controller for both the position and attitude loops of a quadrotor, achieving stabilization of pose within a predetermined time. Yang Weiping [13] identifies the realization of prescribed-time convergence with guaranteed performance for the entire system as a key direction for future research. Meanwhile, Prescribed Performance Control (PPC) methods [14] focus on constraining the tracking error within prespecified bounds. Recent advances have integrated prescribed performance with adaptive control techniques [15], demonstrating improved robustness for nonlinear interconnected systems through event-triggered mechanisms and prespecified-performance-driven strategies. Integrating PTC with PPC offers synergistic advantages but also presents significant challenges: conventional PPC approaches typically employ fixed performance bounds, rendering controller robustness sensitive to initial conditions. When the initial tracking error is large, these bounds often need to be relaxed to avoid constraint violations, thereby degrading transient performance [14]. Specifically, classical PPC methods require the initial condition to satisfy $|z_j(0)| < p(0)$, where $z_j(0)$ is the initial tracking error and $p(0)$ is the initial performance bound. This requirement cannot be guaranteed when initial conditions are arbitrary or unknown, limiting the practical applicability of conventional PPC in scenarios with large initial deviations.

On the other hand, sliding-mode control (SMC) has been extensively applied to quadrotor attitude control due to its finite-time convergence properties [16,17]. However, traditional terminal sliding-mode control suffers from singularity issues, and its convergence time depends on the initial conditions. To mitigate this, Labbadi et al. [18] proposes a nonsingular terminal sliding-mode control method to eliminate singularities, yet the convergence time still cannot be prescribed a priori.

Furthermore, accurate estimation and compensation of disturbances are crucial for enhancing the robustness and tracking accuracy of UAVs. Ding Xilun et al. [19] reviews recent advances in rotorcraft UAV dynamic modeling and disturbance analysis, emphasizing that precise disturbance compensation is pivotal for improving control performance. Liao Jian et al. [20] design a linear extended state observer (LESO) for disturbance estimation, but its estimation accuracy and convergence speed are limited. Cao et al. [21] propose a finite-time disturbance observer, yet its convergence characteristics depend on initial system parameters. Wang et al. [22] develop an adaptive sliding-mode control scheme to enhance robustness and compensate for disturbances. Liu et al. [23] proposed a fixed-time disturbance observer-based control approach for quadcopter suspension transportation systems, demonstrating that fixed-time convergence properties can significantly enhance disturbance rejection performance in payload manipulation tasks with strict temporal requirements. Such fixed-time observer techniques show promise for broader UAV control applications in which rapid, bounded disturbance estimation is essential. Nevertheless, within the domain of QUAV control, approaches that simultaneously account for unknown disturbances, prescribed-time performance guarantees, and highly dynamic initial conditions remain insufficiently investigated.

In summary, existing robust control methods for QUAVs share several common limitations [24]: (1) sensitivity to initial conditions; (2) inefficiency in disturbance estimation and compensation; and (3) lack of precise tracking control with prescribed-time performance bounds. To address these challenges, this paper proposes a trajectory-tracking control scheme for QUAVs that achieves prescribed performance within a prescribed time under highly dynamic initial conditions and in the presence of complex disturbances. Based on a decoupled QUAV dynamic model, we develop a prescribed-time disturbance observer, a position-loop control law (emphasizing precise trajectory tracking), and an attitude-loop control law (emphasizing rapid and robust stabilization). Specifically, to compensate for disturbance effects, an adaptive composite disturbance observer with prescribed-time convergence is designed. For position control, a novel prescribed performance function independent of initial states is proposed based on PPC, along with its corresponding control law. For attitude control, a prescribed-time nonsingular terminal sliding-mode surface and its associated control law are constructed. The main contributions of this work are as follows:

- Initial-condition-independentprescribed performance control: A novel prescribed performance control method that achieves performance constraint satisfaction within a prescribed time regardless of the magnitude of initial tracking errors, addressing a fundamental limitation of conventional prescribed performance control methods that require the initial error to be smaller than the initial performance bound. This is realized through a smooth transition function that decouples the initial error magnitude from the performance bound, transforming the original tracking error into a scaled variable that is inherently small at the initial instant, thereby ensuring satisfaction of the performance constraint for arbitrary initial conditions—a capability not achievable by standard prescribed performance control approaches and directly addressing the robustness requirements highlighted in recent resilient UAV tracking literature [8].

- Prescribed-time convergent nonsingular terminal sliding-mode controller: A controller that enables rapid stabilization of the attitude loop to a small neighborhood of the origin within prescribed time. The prescribed-time convergence property is embedded in the sliding surface design through power-law terms whose coefficients are explicitly derived from the user-specified convergence time parameter, ensuring that the convergence time bound is determined a priori rather than depending on the system's initial state.
- Prescribed-time adaptive disturbance observer: An observer that enhances system robustness and disturbance rejection capability with guaranteed ultimate boundedness within a fixed time.

2. Problem Formulation and Preliminaries

The mathematical model of quadrotor UAVs is primarily based on coordinate transformations and rigid-body dynamics. The dynamic model of quadrotor UAVs is given as [25]

$$\begin{cases} \ddot{x} = [U_1(\cos\varphi\sin\theta\cos\Psi + \sin\varphi\sin\Psi) - K_x\dot{x} + f_x]/m \\ \ddot{y} = [U_1(\cos\varphi\sin\theta\sin\Psi - \sin\varphi\cos\Psi) - K_y\dot{y} + f_y]/m \\ \ddot{z} = [U_1(\cos\varphi\cos\theta) - mg - K_z\dot{z} + f_z]/m \\ \ddot{\varphi} = [U_2 + (I_y - I_z)\dot{\theta}\dot{\Psi} - K_\varphi\omega_\varphi + f_\varphi]/I_x \\ \ddot{\theta} = [U_3 + (I_z - I_x)\dot{\varphi}\dot{\Psi} - K_\theta\omega_\theta + f_\theta]/I_y \\ \ddot{\Psi} = [U_4 + (I_x - I_y)\dot{\varphi}\dot{\theta} - K_\Psi\omega_\Psi + f_\Psi]/I_z \end{cases} \tag{1}$$

where (U_1, U_2, U_3, U_4) are the motor torques that govern the three position coordinates (x, y, z) and three attitude angles (φ, θ, Ψ) of the quadrotor UAVs; $I_i (i = x, y, z)$ represent the moments of inertia about the x, y, and z-axes of the body coordinate system, $f_i (i = x, y, z, \theta, \varphi, \Psi)$ refer to disturbances; and $K_i (i = x, y, z, \theta, \varphi, \Psi)$ represent the aerodynamic drag coefficients. Additionally, m represents the mass of the quadrotor, and g is the acceleration of gravity. In the dynamic model, U_1 is allocated to the displacements along the x, y and z directions such that the entire quadrotor control system can be decomposed into a position control system governed by U_1 and an attitude control system controlled by U_2, U_3 and U_4. For the purpose of feedback linearization, the virtual control inputs along the x, y and z directions (u_x, u_y, u_z) are introduced as [25]:

$$\begin{cases} u_x = [U_1(\cos\varphi\sin\theta\cos\Psi + \sin\varphi\sin\Psi)]/m \\ u_y = [U_1(\cos\varphi\sin\theta\sin\Psi - \sin\varphi\cos\Psi)]/m \\ u_z = [U_1(\cos\varphi\cos\theta - mg)]/m \end{cases} \tag{2}$$

Based on the dynamic model of the quadrotor UAVs and the specified desired yaw angle Ψ_d, along with the three virtual control inputs, the desired roll angle, pitch angle, and thrust U_1 can be determined as follows [20]:

$$\begin{cases} U_1 = m\sqrt{u_x^2 + u_y^2 + (u_z + g)^2} \\ \varphi_d = \arcsin\left[\frac{m(u_x\sin\Psi_d - u_y\cos\Psi_d)}{U_1}\right] \\ \theta_d = \arctan\left[\frac{m(u_x\cos\Psi_d + u_y\sin\Psi_d)}{m(u_z+g)}\right] \end{cases} \tag{3}$$

Remark 1. *To avoid domain violations in the arcsin function, saturation protection is implemented in practice:*

$$\varphi_d = \arcsin\left[sat\left(\frac{m(u_x\sin\Psi_d - u_y\cos\Psi_d)}{U_1}, -0.99, 0.99\right)\right]$$

where $sat(x, a, b) = \max(a, \min(b, x))$.

The objective of this paper is to design control laws for QUAVs achieving prescribed performance bounds and prescribed-time satisfaction under arbitrary initial conditions. To theoretically guarantee the robust performance of the proposed control law, the following lemma is introduced.

Lemma 1 ([26]). *For a general smooth nonlinear system in the form of*

$$\dot{x} = f(x), f(0) = 0, x \in R^n \tag{4}$$

If there is a continuous function $V(x)$ that satisfies

$$\dot{V}(x) \leq -\left(\pi/\gamma T_c \sqrt{\alpha\beta}\right)\left(\alpha V^{(1-\gamma/2)}(x) + \beta V^{(1+\gamma/2)}(x)\right), \tag{5}$$

where $\alpha > 0, \beta > 0, 0 < \gamma < 1$ and $T_c > 0$, then system (4) is globally prescribed-time stable, i.e., $V(x)$ converges to a small neighborhood of the origin within prescribed time T_C.

Lemma 2 (Properties of Hyperbolic Tangent Function). *For the hyperbolic tangent function* $\tanh : \mathbb{R} \to (-1, 1)$, *the following properties hold:*

(i) $x \tanh(x) > 0$ *for all* $x \neq 0$;

(ii) $\tanh(x)$ *is strictly increasing and odd:* $\tanh(-x) = -\tanh(x)$;

(iii) $0 < \frac{\tanh(x)}{x} < 1$ *for all* $x \neq 0$;

(iv) $\lim_{x\to 0} \frac{\tanh(x)}{x} = 1$.

Proof. Property (i) follows from $\tanh(x) = \frac{e^x - e^{-x}}{e^x + e^{-x}}$ having the same sign as x.

Property (ii): $\frac{d}{dx}\tanh(x) = \operatorname{sech}^2(x) = \frac{4}{(e^x + e^{-x})^2} > 0$, and the odd property is immediate from the definition.

Property (iii): For $x > 0$, since $e^{2x} > 1 + 2x$, we have $\tanh(x) = \frac{e^{2x}-1}{e^{2x}+1} < \frac{e^{2x}-1}{2} < x$. The lower bound follows from $\tanh(x) > 0$ for $x > 0$.

Property (iv) follows from L'Hôpital's rule or the Taylor series $\tanh(x) = x - \frac{x^3}{3} + O(x^5)$. □

3. Prescribed-Time Adaptive Composite Disturbance Observer Design and Analysis

To effectively counteract the effect of unknown disturbances on the QUAVs, a composite disturbance observer with prescribed-time convergence and adaptive mechanisms is introduced in this section. The observer design employs an auxiliary system (Equation (8)) that serves as a virtual reference to enable indirect disturbance estimation. By defining the auxiliary error $e_i = v_i - \vartheta_i$ and designing its adaptive law (Equation (12)), we convert the disturbance estimation problem into a stabilization problem for $\tilde{e}_i$, for which prescribed-time convergence can be rigorously guaranteed via Lemma 1. This auxiliary system technique is analogous to classical extended state observer (ESO) design but with prescribed-time convergence guarantees.

First, note that the drone model can be rewritten as follows:

$$\dot{v}_i = u_i + d_i, i = x, y, z, \varphi, \theta, \Psi, \tag{6}$$

where

$$\begin{cases} v_x = \dot{x}, \\ v_y = \dot{y}, \\ v_z = \dot{z} \end{cases}$$
$$\begin{cases} v_\varphi = \dot{\varphi}, \\ v_\theta = \dot{\theta}, \\ v_\psi = \dot{\psi} \end{cases}$$
$$\begin{cases} u_\varphi = U_2 I_x^{-1}, \\ u_\theta = U_3 I_y^{-1}, \\ u_\psi = U_4 I_z^{-1} \end{cases} \tag{7}$$
$$\begin{cases} d_x = f_x m^{-1} - K_x m^{-1} \dot{x}, \\ d_y = f_y m^{-1} - K_y m^{-1} \dot{y}, \\ d_z = f_z m^{-1} - K_z m^{-1} \dot{z} \end{cases}$$
$$\begin{cases} d_\varphi = f_\varphi - K_\varphi \omega_\varphi I_x^{-1}, \\ d_\theta = f_\theta I_y^{-1} - K_\theta \omega_\theta I_y^{-1}, \\ d_\psi = f_\psi I_z^{-1} - K_\psi \omega_\psi I_z^{-1} \end{cases}$$

By defining auxiliary systems as

$$\dot{\vartheta}_i = u_i + e_i, \tag{8}$$

where the auxiliary error is defined as: $e_i = v_i - \vartheta_i$, the relationship between auxiliary error and disturbance is established as follows. Taking the time derivative of $e_i = v_i - \vartheta_i$ and substituting Equations (6) and (8):

$$\dot{e}_i = \dot{v}_i - \dot{\vartheta}_i = (u_i + d_i) - (u_i + e_i) = d_i - e_i \tag{9}$$

This identity is crucial for the observer design. The prescribed-time adaptive composite disturbance observer is designed as follows [27]:

$$\widehat{d}_i = \widehat{e}_i + \dot{e}_i \tag{10}$$

Substituting $\dot{e}_i = d_i - e_i$:

$$\hat{d}_i = \hat{e}_i + d_i - e_i$$

Therefore, the observation error becomes the following:

$$\tilde{d}_i = d_i - \hat{d}_i = d_i - (\hat{e}_i + d_i - e_i) = e_i - \hat{e}_i = \tilde{e}_i \tag{11}$$

where the adaptive law follows that

$$\dot{\hat{e}}_i = \dot{e}_i + a_1 \operatorname{sign}(\widetilde{e}_i)|\widetilde{e}_i|^{1-\gamma_1} + a_2 \operatorname{sign}(\widetilde{e}_i)|\widetilde{e}_i|^{1+\gamma_1} + a_3 \tanh(\widetilde{e}_i), \tag{12}$$

in which parameters satisfy the following:

$$a_1 = \frac{\pi \eta_1^{1/2}}{\gamma_1 T_1 \beta_1^{1/2}} \left(\frac{1}{2}\right)^{1-\frac{\gamma_1}{2}}, a_2 = \frac{\pi \beta_1^{1/2}}{\gamma_1 T_1 \eta_1^{1/2}} \left(\frac{1}{2}\right)^{1+\frac{\gamma_1}{2}},$$

$$a_3 > 0, \gamma_1 \in (0,1), \eta_1 > 0, \beta_1 > 0$$

To demonstrate the performance of the disturbance observer analytically, the adaptive estimation error is defined as follows:

$$\widetilde{e}_i = e_i - \widehat{e}_i \tag{13}$$

Then, the derivative of the auxiliary error can be shown to satisfy the following:

$$\dot{\widetilde{e}}_i = -a_1 \operatorname{sign}(\widetilde{e}_i)|\widetilde{e}_i|^{1-\gamma_1} - a_2 \operatorname{sign}(\widetilde{e}_i)|\widetilde{e}_i|^{1+\gamma_1} - a_3 \tanh(\widetilde{e}_i) \tag{14}$$

Now, consider candidate Lyapunov functions given as follows:

$$\bar{V}_i = \frac{1}{2}\widetilde{e}_i^2 \tag{15}$$

The derivative of $\bar{V}_i$ is as follows:

$$\begin{aligned} \dot{\bar{V}}_i &= \tilde{e}_i \dot{\tilde{e}}_i \\ &= -a_1|\tilde{e}_i|^{2-\gamma_1} - a_2|\tilde{e}_i|^{2+\gamma_1} - a_3\tilde{e}_i \tanh(\tilde{e}_i) \end{aligned} \tag{16}$$

By Lemma 2(i), $\tilde{e}_i \tanh(\tilde{e}_i) \geq 0$ for all $\tilde{e}_i \in \mathbb{R}$. Therefore,

$$\dot{\bar{V}}_i \leq -a_1|\tilde{e}_i|^{2-\gamma_1} - a_2|\tilde{e}_i|^{2+\gamma_1}. \tag{17}$$

Using $|\tilde{e}_i| = (2\bar{V}_i)^{1/2}$,

$$\begin{aligned} \dot{\bar{V}}_i &\leq -a_1(2\bar{V}_i)^{\frac{2-\gamma_1}{2}} - a_2(2\bar{V}_i)^{\frac{2+\gamma_1}{2}} \\ &= -a_1 2^{\frac{2-\gamma_1}{2}} \bar{V}_i^{1-\frac{\gamma_1}{2}} - a_2 2^{\frac{2+\gamma_1}{2}} \bar{V}_i^{1+\frac{\gamma_1}{2}} \end{aligned} \tag{18}$$

By the parameter selection, we have the following:

$$a_1 2^{\frac{2-\gamma_1}{2}} = \frac{\pi\eta_1^{1/2}}{\gamma_1 T_1 \beta_1^{1/2}}, \quad a_2 2^{\frac{2+\gamma_1}{2}} = \frac{\pi\beta_1^{1/2}}{\gamma_1 T_1 \eta_1^{1/2}}$$

Therefore,

$$\dot{\bar{V}}_i \leq -\frac{\pi}{\gamma_1 T_1 \sqrt{\eta_1\beta_1}}\left(\eta_1 \bar{V}_i^{1-\frac{\gamma_1}{2}} + \beta_1 \bar{V}_i^{1+\frac{\gamma_1}{2}}\right). \tag{19}$$

According to Lemma 1, $\widetilde{e}_i$ converges to a small neighborhood of the origin within a prescribed time T_1 when disturbances are constant. Since $\widetilde{d}_i = \widetilde{e}_i$, the observer can estimate constant composite disturbances within prescribed time T_1.

Remark 2. *The term $-a_3\tilde{e}_i \tanh(\tilde{e}_i)$ is always non-positive by Lemma 2(i), which strictly enhances the convergence rate. However, it does not contribute to the prescribed-time mechanism, which is solely determined by the power terms with exponents $1-\gamma_1/2$ and $1+\gamma_1/2$.*

Theorem 1. *(Ultimate Boundedness under Time-Varying Disturbances)*

Consider the disturbance observer (8)–(12) with time-varying disturbances $d_i(t)$ satisfying the following:

$$|\dot{d}_i(t)| \leq D_{\max}, \quad \forall t \geq 0$$

Then for any $\varepsilon > 0$, if $a_3 > \frac{2D_{\max}}{\varepsilon}$, there exists a finite time $T_\varepsilon \geq T_1$ such that

$$|\tilde{d}_i(t)| \leq \varepsilon, \quad \forall t \geq T_\varepsilon$$

Proof. From Equation (14):

$$\dot{\tilde{d}}_i = -a_1 \text{sign}(\tilde{d}_i)|\tilde{d}_i|^{1-\gamma_1} - a_2 \text{sign}(\tilde{d}_i)|\tilde{d}_i|^{1+\gamma_1} - a_3 \tanh(\tilde{d}_i) + \dot{d}_i$$

Consider the set $\mathcal{S}_\varepsilon = \{x \in \mathbb{R} : |x| \leq \varepsilon\}$.
At the boundary $|\tilde{d}_i| = \varepsilon$, assume without loss of generality $\tilde{d}_i = \varepsilon > 0$:

$$\dot{\tilde{d}}_i\big|_{\tilde{d}_i=\varepsilon} \leq -a_1\varepsilon^{1-\gamma_1} - a_2\varepsilon^{1+\gamma_1} - a_3 \tanh(\varepsilon) + D_{\max}$$

For small ε, using Lemma 2(iv), $\tanh(\varepsilon) \geq \varepsilon/2$ (by continuity). A sufficient condition for $\mathcal{S}_\varepsilon$ to be positively invariant is as follows:

$$a_3 \cdot \frac{\varepsilon}{2} > D_{\max}$$

which gives $\varepsilon > \frac{2D_{\max}}{a_3}$.

For any initial $\tilde{d}_0$ outside $\mathcal{S}_\varepsilon$, finite-time reaching is guaranteed by the dominant power terms, with reaching time bounded by $T_\varepsilon - T_1 \leq \tilde{d}_0^2/(2\delta)$ for some $\delta > 0$. □

4. Prescribed-Time Controller Design for QUAVs

Based on the estimate of disturbance from the aforementioned disturbance observer, this section develops a QUAVs' controller ensuring robust and accurate tracking with prescribed-time performance satisfaction. The hierarchical control structure is illustrated in Figure 1, which shows the outer position loop generating virtual controls (u_x, u_y, u_z) via the PPC-based controller, the coordinate transformation converting these to desired attitude angles (φ_d, θ_d) and thrust U_1, the inner attitude loop using the NTSM controller to generate motor torques (U_2, U_3, U_4), and the disturbance observer providing estimates $\hat{d}_i$ to both controllers. (The solid line represents the real signal, and the dashed line represents the virtual signal).

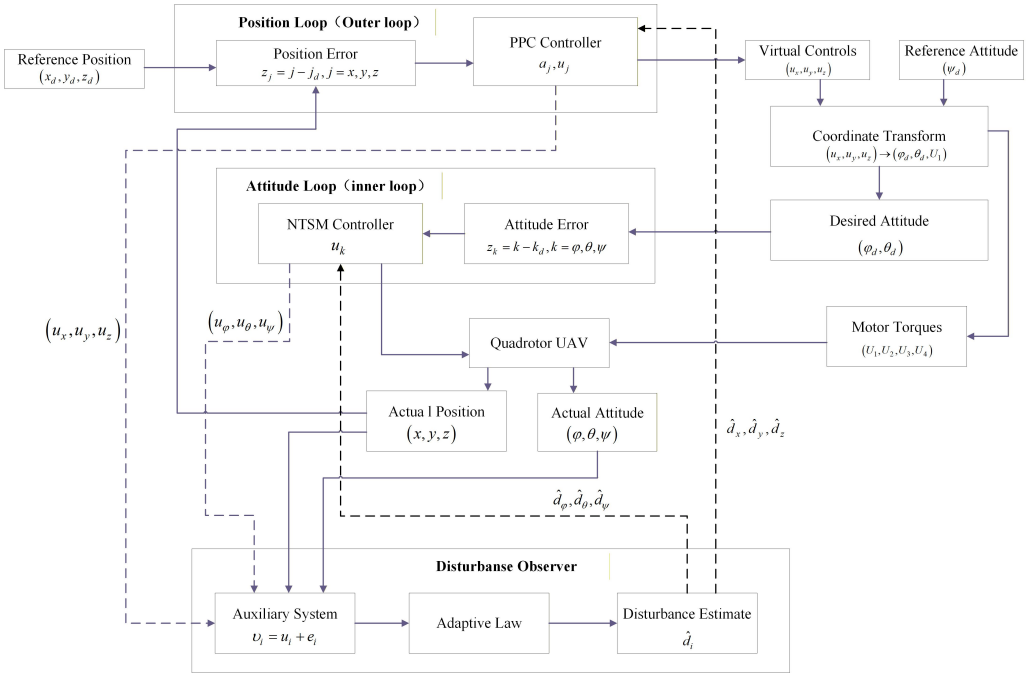


Figure 1. Overall Architecture of the Proposed Control Scheme.

4.1. Design of Prescribed-Time and Prescribed-Performance Controller for Position Loop

First, a prescribed-time control law for position control is designed for robust tracking. To accomplish the position system control objective, the position tracking error of the QUAVs is defined as follows:

$$z_x = x - x_d,\ z_y = y - y_d,\ z_z = z - z_d \tag{20}$$

where $[z_x, z_y, z_z]^T$ represents the position tracking error vector, $[x_d, y_d, z_d]^T$ includes the desired reference values for the three position components, and the actual output values for the three position components are $[x, y, z]^T$. The prescribed performance function can be designed as follows [28]:

$$p(t) = \begin{cases} \left(p_0 - \frac{t}{T_2}\right)\exp\left(1 - \frac{t}{T_2 - t}\right) + p_\infty, 0 \le t < T_2 \\ p_\infty, t \ge T_2 \end{cases} \tag{21}$$

where $p_0 > 1$ and p_∞ are design parameters, and T_2 is a prescribed time parameter.

To render the prescribed performance control independent of initial conditions, the following function is introduced [29]:

$$\xi = \begin{cases} \xi_0 + (1 - \xi_0)\frac{1 - \cos(\frac{\pi t}{T_2})}{2}, t < T_2 \\ 1, t \ge T_2 \end{cases} \tag{22}$$

Remark 3. *The smooth cosine transition function $\xi(t)$ with $\xi(0) = \xi_0 \approx 0$ (e.g., $\xi_0 = 0.001$) ensures: (1) Initial-condition decoupling: The transformed error $s_{j1}(0) = \xi_0 z_j(0)$ becomes arbitrarily small regardless of the magnitude of $z_j(0)$, guaranteeing $|s_{j1}(0)| < p(0)$ for any initial tracking error. (2) Continuity of control: The function satisfies $\xi(t) \in C^\infty$ for all $t \ge 0$, with $\dot{\xi}(t) = \frac{\pi(1-\xi_0)}{2T_2}\sin(\frac{\pi t}{T_2})$ continuous at $t = T_2$ (where $\dot{\xi}(T_2^-) = 0 = \dot{\xi}(T_2^+)$), eliminating discontinuities in control terms containing $\dot{\xi}$. For $t < T_2$, while $s_{j1} = \xi z_j$ grows with $\xi(t)$, the simultaneous decay of the performance bound $p(t)$ ensures that the constraint $|s_{j1}| < p(t)$ is maintained, which in turn bounds the physical error as $|z_j| < p(t)/\xi(t)$.*

Then if we define

$$\begin{cases} s_{x1} = \xi z_x, s_{x2} = \dot{x} - \alpha_x \\ s_{y1} = \xi z_y, s_{y2} = \dot{y} - \alpha_y \\ s_{z1} = \xi z_z, s_{z2} = \dot{z} - \alpha_z \end{cases}, \tag{23}$$

it follows that their derivatives satisfy the following:

$$\begin{cases} \dot{s}_{x1} = \dot{\xi} z_x + \xi(\dot{x} - \dot{x}_d), \dot{s}_{x2} = u_x + d_x - \dot{\alpha}_x \\ \dot{s}_{y1} = \dot{\xi} z_y + \xi(\dot{y} - \dot{y}_d), \dot{s}_{y2} = u_y + d_y - \dot{\alpha}_y \\ \dot{s}_{z1} = \dot{\xi} z_z + \xi(\dot{z} - \dot{z}_d), \dot{s}_{z2} = u_z + d_z - \dot{\alpha}_z \end{cases}. \tag{24}$$

Note that if the control law is designed such that

$$-p(t) < s_{j1} < p(t), j = x, y, z \tag{25}$$

it follows from $\xi(0) = \xi_0 \approx 0$ that $s_{j1}(0) = \xi_0 z_j(0) \approx 0$, which implies that $-p(0) < s_{j1}(0) < p(0)$ can be satisfied regardless of the value of $z_j(0)$, and after $T_2, s_j = \xi z_j$ always holds true.

To achieve the desired performance constraints, consider candidate Lyapunov functions with barriers designed as follows [29]:

$$V_{j1} = \frac{1}{2}\ln\frac{p^2}{p^2 - s_{j1}^2},\ (j = x, y, z).$$

Lemma 3 (Boundedness of barrier Lyapunov function components)**.** *For the barrier Lyapunov function* $V_{j1} = \frac{1}{2}\ln\frac{p^2}{p^2-s_{j1}^2}$ *with* $|s_{j1}| < p$*, the following properties hold:*

(i) The normalized error satisfies the following:

$$\frac{s_{j1}^2}{p^2 - s_{j1}^2} \geq 2V_{j1}$$

(ii) When $|s_{j1}| < p$*, there exist positive constants* $\underline{\ell}_j$ *and* $\overline{\ell}_j$ *such that*

$$\underline{\ell}_j \leq \left|\frac{s_{j1}}{p^2 - s_{j1}^2}\right| \leq \overline{\ell}_j.$$

(iii) For the performance function $p(t)$ *defined in (21), there exists a constant* $\overline{M}_p > 0$ *such that*

$$\left|\frac{\dot{p}(t)}{p(t)}\right| \leq \overline{M}_p, \quad \forall t \geq 0.$$

Proof. (i) From the definition, $e^{2V_{j1}} = \frac{p^2}{p^2-s_{j1}^2}$, which yields the following:

$$p^2 - s_{j1}^2 = p^2 e^{-2V_{j1}}$$

Therefore,

$$\frac{s_{j1}^2}{p^2 - s_{j1}^2} = \frac{p^2 - (p^2 - s_{j1}^2)}{p^2 - s_{j1}^2} = e^{2V_{j1}} - 1 \geq 2V_{j1}$$

where the last inequality follows from $e^x \geq 1 + x$ for all $x \in \mathbb{R}$.

(ii) Since $|s_{j1}| < p$ is maintained by the barrier, and $p(t) \geq p_\infty > 0$, the function $\ell_j(t) = \frac{s_{j1}}{p^2-s_{j1}^2}$ is bounded.

(iii) Computing $\dot{p}(t)$ from (20) for $t < T_2$:

$$\dot{p}(t) = -\frac{1}{T_2}\exp\left(1 - \frac{t}{T_2 - t}\right) + (p_0 - \frac{t}{T_2})\exp\left(1 - \frac{t}{T_2 - t}\right) \cdot \frac{T_2}{(T_2 - t)^2}.$$

Since $p(t) \geq p_\infty$, the ratio $|\dot{p}/p|$ remains bounded for all $t \geq 0$. □

It follows that

$$\begin{aligned} \dot{V}_{j1} &= \tfrac{s_{j1}}{p^2-s_{j1}^2}\left(\dot{s}_{j1} - \dot{p}s_{j1}/p\right) \\ &= \ell_j\left(\dot{\xi}z_j + \xi\left(s_{j2} + \alpha_j - \dot{j}_d\right) - \dot{p}s_{j1}/p\right) \\ &= \ell_j\xi\left(s_{j2} + \alpha_j - \dot{j}_d\right) + \ell_j\left(\dot{\xi}z_j - \dot{p}s_{j1}/p\right), \end{aligned} \tag{26}$$

where $\ell_j = \frac{s_{j1}}{p^2-s_{j1}^2}$.

According to Young's inequality, for any $\lambda_j > 0$, we have the following:

$$-\ell_j\dot{p}s_{j1}/p \leq \frac{\ell_j^2 s_{j1}^2}{2\lambda_j}\frac{\dot{p}^2}{p^2} + \frac{\lambda_j}{2}$$

By Lemma 3(ii) and (iii), there exists $\rho_{j1} > 0$ such that

$$\frac{\ell_j^2 s_{j1}^2}{2\lambda_j}\frac{\dot{p}^2}{p^2} \le \rho_{j1}$$

for all $t \ge 0$ and all $|s_{j1}| < p$.

By plugging it into (26), we can obtain the following:

$$\dot{V}_{j1} \le \ell_j \xi \left(s_{j2} + \alpha_j - \dot{j}_d + \frac{\ell_j \xi z_j^2}{2\lambda_j}\frac{\dot{p}^2}{p^2} \right) + \rho_{j1} + \frac{\lambda_j}{2} + \ell_j \dot{\xi} z_j \tag{27}$$

By designing the position loop virtual control rate as

$$\alpha_j = -\mu_{j1} s_{j1} + \dot{j}_d - \frac{\ell_j \xi z_j^2}{2\lambda_j}\frac{\dot{p}^2}{p^2}, \tag{28}$$

where μ_{j1} is the regularization parameter, it follows from (27) that

$$\dot{V}_{j1} \le -\mu_{j1}\xi \frac{s_{j1}^2}{p^2 - s_{j1}^2} + \rho_{j1} + \frac{\lambda_j}{2} + \ell_j \xi s_{j2} + \ell_j \dot{\xi} z_j.$$

To further design the stabilizing control law, let us consider candidate Lyapunov functions given as $V_{j2} = V_{j1} + \frac{1}{2}s_{j2}^2$, whose derivatives satisfy the following:

$$\dot{V}_{j2} = \dot{V}_{j1} + s_{j2}\dot{s}_{j2} = \dot{V}_{j1} + s_{j2}(u_j + d_j - \dot{\alpha}_j) \tag{29}$$

To eliminate the problematic singular term, we employ the following continuous approximation. Note that

$$\ell_j \dot{\xi} z_j s_{j2} = \ell_j \dot{\xi} z_j s_{j2} \cdot \frac{s_{j2}^2 + \delta_j^2}{s_{j2}^2 + \delta_j^2},$$

where $\delta_j > 0$ is a small design parameter. This allows us to write the following:

$$\ell_j \dot{\xi} z_j = \ell_j \dot{\xi} z_j \cdot \frac{s_{j2}}{s_{j2}^2 + \delta_j^2} \cdot s_{j2}$$

The control law is thus designed as follows:

$$u_j = -\mu_{j2} s_{j2} - \widehat{d}_j + \dot{\alpha}_j - \ell_j \xi - \ell_j \dot{\xi} z_j \frac{s_{j2}}{s_{j2}^2 + \delta_j^2}, \tag{30}$$

where $\mu_{j2}(j = x, y, z)$ is the regularization parameter and $\delta_j > 0$ is a small positive constant that prevents singularity when $s_{j2} \to 0$.

Remark 4. *The continuous approximation* $\frac{s_{j2}}{s_{j2}^2+\delta_j^2}$ *ensures the following: (1) The control law remains bounded for all* s_{j2}*, including* $s_{j2} = 0$*; (2) When* $|s_{j2}| \gg \delta_j$*, the approximation* $\frac{s_{j2}}{s_{j2}^2+\delta_j^2} \approx s_{j2}^{-1}$ *closely matches the original design intent; (3) The approximation error* $\ell_j \dot{\xi} z_j \frac{\delta_j^2}{s_{j2}^2+\delta_j^2}$ *is uniformly bounded and can be made arbitrarily small by choosing* δ_j *sufficiently small, while maintaining control continuity.*

https://doi.org/10.3390/electronics15020408

Theorem 2. *Consider the quadrotor UAV position subsystem described by (6) with the prescribed-time disturbance observer (8)–(12) and the position control law (19)–(30). Suppose the following conditions hold:*

1. *The desired trajectory is bounded and twice differentiable;*
2. *The observer parameters satisfy* $\alpha > 0,\ \beta > 0,\ 0 < \gamma < 1$;
3. *The controller parameter* $p_0 > 1$;
4. *The prescribed time parameters satisfy* $T_1 > 0,\ T_2 > 0$; *and the approximation parameter* $\delta_j > 0$.

Then, the position tracking error converges to a small neighborhood of the prescribed performance bounds within the prescribed time, specifically: (i) the performance constraint $|s_{j1}(t)| < p(t)$ *is satisfied for all* $t \geq 0$, *ensuring* $|z_j(t)| < p(t)/\xi(t)$; *and (ii) for* $t \geq T_2$, *the system exhibits exponential ultimate boundedness with* $|z_j(t)| \leq p_\infty + \mathcal{O}(\sqrt{\Theta_j/\mu_j})$, *where the bound* Θ_j *depends on disturbance observation error, control approximation error, and performance function derivative.*

Remark 5. *The term "arbitrary initial conditions" in this paper refers to a theoretical framework where the control method can handle a wide range of initial states. In practical UAV applications, the initial conditions are naturally constrained by physical limitations. Therefore, "arbitrary initial conditions" should be interpreted as "high-redundancy initial conditions".*

Proof. Substituting the control law (30) into (29):

$$\dot{V}_{j2} \leq -\mu_{j1}\xi\frac{s_{j1}^2}{p^2-s_{j1}^2} - \mu_{j2}s_{j2}^2 + \rho_{j1} + \frac{\lambda_j}{2} + \ell_j\dot{\xi}z_j\frac{\delta_j^2}{s_{j2}^2+\delta_j^2} + s_{j2}\tilde{d}_j \tag{31}$$

Using Young's inequality on $s_{j2}\tilde{d}_j$:

$$s_{j2}\tilde{d}_j \leq \frac{s_{j2}^2}{2\epsilon_j} + \frac{\epsilon_j\tilde{d}_j^2}{2}$$

and noting that $\frac{\delta_j^2}{s_{j2}^2+\delta_j^2} \leq 1$ and by Lemma 3(ii) $|\ell_j| \leq \bar{\ell}_j$, we have the following:

$$\ell_j\dot{\xi}z_j\frac{\delta_j^2}{s_{j2}^2+\delta_j^2} \leq \bar{\ell}_j|\dot{\xi}||z_j| \leq \rho_{j2}$$

for some constant $\rho_{j2} > 0$ (since $\dot{\xi}$ and z_j remain bounded in the closed-loop system).

Therefore,

$$\dot{V}_{j2} \leq -\mu_{j1}\xi\frac{s_{j1}^2}{p^2-s_{j1}^2} - \left(\mu_{j2} - \frac{1}{2\epsilon_j}\right)s_{j2}^2 + \Theta_j, \tag{32}$$

where $\Theta_j = \rho_{j1} + \rho_{j2} + \frac{\lambda_j}{2} + \frac{\epsilon_j D_{\max}^2}{2}$ (using the bound from Theorem 1 on $|\tilde{d}_j| \leq \varepsilon$ for sufficiently large t).

By Lemma 3(i):

$$\begin{aligned}\dot{V}_{j2} &\leq -2\mu_{j1}\xi V_{j1} - \left(\mu_{j2} - \tfrac{1}{2\epsilon_j}\right)s_{j2}^2 + \Theta_j \\ &\leq -\mu_j V_{j2} + \Theta_j\end{aligned} \tag{33}$$

where $\mu_j = \min\left\{2\mu_{j1}\xi_{\min}, 2\left(\mu_{j2} - \frac{1}{2\epsilon_j}\right)\right\} > 0$ (provided $\mu_{j2} > \frac{1}{2\epsilon_j}$, which can be satisfied by design), and $\xi_{\min} = \xi_0 > 0$ is the minimum value of $\xi(t)$. By integrating both sides of (33), we have the following:

$$V_{j2} \leq \left(V_{j2}(0) - \frac{\Theta_j}{\mu_j} \right) \exp(-\mu_j t) + \frac{\Theta_j}{\mu_j} \tag{34}$$

By substituting the aforementioned expression into Equation (33), it can be inferred that $\dot{V}_{j2} \leq 0$. Since

$$\begin{aligned} V_{j2} &= V_{j1} + (1/2){s_{j2}}^2 = (1/2)\ln\left[p^2/\left(p^2 - {s_{j1}}^2\right)\right] + 1/2{s_{j2}}^2 \\ &\leq Ae^{\left(-\mu_j t\right)} + B, \end{aligned}$$

where $A = V_{j2}(0) - \frac{\Theta_j}{\mu_j}$, $B = \frac{\Theta_j}{\mu_j}$, then

$$\begin{aligned} &\ln\left[p^2/\left(p^2 - s_{j1}^2\right)\right] \leq 2Ae^{\left(-\mu_j t\right)} + 2B \\ &p^2/\left(p^2 - s_{j1}^2\right) \leq e^{2Ae^{\left(-\mu_j t\right)} + 2B} \\ &C(t){s_{j1}}^2 \leq (C(t) - 1)p^2 \end{aligned}$$

in which $C(t) = e^{2Ae^{\left(-\mu_j t\right)} + 2B}$. Therefore, ${s_{j1}}^2 \leq p^2$. In this case, prescribed performance $-p(t) < s_{j1} < p(t)$ holds, and the system states converge to a small neighborhood of the origin. □

Remark 6. *(Clarification on Performance Satisfaction)*

The proposed method achieves two distinct aspects:

(i) Prescribed-time performance constraint satisfaction: The barrier Lyapunov function guarantees $|s_{j1}(t)| < p(t)$ for all $t \geq 0$, where $p(t)$ decreases from p_0 to p_∞ within time T_2. This ensures the physical tracking error satisfies $|z_j(t)| < p(t)/\xi(t)$, achieving bounded tracking within the prescribed time T_2 regardless of initial conditions.

(ii) Exponential ultimate boundedness: The inequality $\dot{V}_{j2} \leq -\mu_j V_{j2} + \Theta_j$ (Equation (33)) yields exponential convergence to an ultimate bound $\lim_{t\to\infty} V_{j2}(t) \leq \Theta_j/\mu_j$, rather than exact convergence to zero. The bound Θ_j arises from three sources: (a) disturbance observation error $|\tilde{d}_j| \leq \varepsilon$ (Theorem 1), (b) continuous approximation error ρ_{j2} from the term $\delta_j^2/(s_{j2}^2 + \delta_j^2)$ (Equation (30)), and (c) performance function derivative bound ρ_{j1} (Lemma 3).

(iii) Engineering rationale for $p_\infty > 0$: Setting $p_\infty = 0$ would theoretically require infinite control gains at $t = T_2$, which is impractical given actuator saturation. The design choice $p_\infty > 0$ provides the following: (a) bounded control effort, (b) robustness to persistent disturbances and modeling uncertainties, and (c) adjustable steady-state accuracy through parameter tuning (a_3, δ_j, ϵ_j, μ_j). The ultimate bound can be made arbitrarily small by appropriate parameter selection.

4.2. Design of Sliding Mode Controller for Prescribed-Time Attitude Loop

Considering the characteristics of the QUAV's attitude dynamics, applying a prescribed-time terminal sliding mode controller that is different from the controller used for the position loop can be more effective for rapid and robust stabilization of the attitude loop.

To design and analyze the controller, the errors in attitude tracking of a quadrotor UAV are defined as follows:

$$z_\varphi = \varphi - \varphi_d,\ z_\theta = \theta - \theta_d,\ z_\Psi = \Psi - \Psi_d, \tag{35}$$

where $[\varphi_d, \theta_d, \Psi_d]^T$ is the reference attitude input vector, and $[\varphi, \theta, \Psi]^T$ is the actual output attitude angle information. The derivatives of errors in (35) can be obtained by the following:

$$\dot{z}_\varphi = \dot{\varphi} - \dot{\varphi}_d,\ \dot{z}_\theta = \dot{\theta} - \dot{\theta}_d,\ \dot{z}_\Psi = \dot{\Psi} - \dot{\Psi}_d \tag{36}$$

where $\left[\dot{z}_\varphi, \dot{z}_\theta, \dot{z}_\Psi\right]^T$, $\left[\dot{\varphi}_d, \dot{\theta}_d, \dot{\Psi}_d\right]^T$, and $\left[\dot{\varphi}, \dot{\theta}, \dot{\Psi}\right]^T$ represent the derivatives of $\left[z_\varphi, z_\theta, z_\Psi\right]^T$, $[\varphi_d, \theta_d, \Psi_d]^T$, and $[\varphi, \theta, \Psi]^T$, respectively.

The prescribed-time non-singular terminal sliding mode surface for the attitude control system is designed as [26]:

$$s_k = \dot{z}_k + b_1 \operatorname{sign}(z_k)|z_k|^{1-\gamma_2} + b_2 \operatorname{sign}(z_k)|z_k|^{1+\gamma_2} (k = \varphi, \theta, \Psi) \tag{37}$$

where the parameters satisfy the following:

$$b_1 = \frac{\pi \eta_2^{1/2}}{\gamma_2 T_3 \beta_2^{1/2}} \left(\frac{1}{2}\right)^{1-\frac{\gamma_2}{2}}, b_2 = \frac{\pi \beta_2^{1/2}}{\gamma_2 T_3 \eta_2^{1/2}} \left(\frac{1}{2}\right)^{1+\frac{\gamma_2}{2}},$$
$$\gamma_2 \in (0,1), \eta_2 > 0, \beta_2 > 0.$$

Remark 7. *The prescribed-time property is directly embedded in the sliding surface design (Equation (37)) through the power-law coefficients b_1 and b_2, which are explicitly functions of the prescribed time T_3. Specifically, when the system reaches the sliding surface $s_k = 0$, the dynamics become the following:*

$$\dot{z}_k + b_1 sign(z_k)|z_k|^{1-\gamma_2} + b_2 sign(z_k)|z_k|^{1+\gamma_2} = 0$$

The above formulation for the sliding mode surface structure, combined with the specific parameter selection of b_1 and b_2, guarantees convergence from any point on the sliding surface to a neighborhood of the origin within time T_3, as proven in Theorem 3.

It can be derived that

$$\dot{s}_k = u_k + d_k - \ddot{k}_d + \varsigma_k \dot{z}_k, \tag{38}$$

where $\varsigma_k = (1-\gamma_2) b_1 |z_k|^{-\gamma_2} + (1+\gamma_2) b_2 |z_k|^{\gamma_2}$.

To design the control law and guarantee stability, consider candidate Lyapunov functions defined as $V_k = \frac{1}{2} s_k^2, k = \varphi, \theta, \Psi$. The derivatives of these functions satisfy the following:

$$\dot{V}_k = s_k \left(u_k + d_k - \ddot{k}_d + \varsigma_k \dot{z}_k\right) \tag{39}$$

Now, we are motivated to design the observer-based sliding mode controller as follows:

$$u_k = I_j \begin{pmatrix} -c_1 \operatorname{sign}(s_k)|s_k|^{1-\gamma_3} - \\ c_2 \operatorname{sign}(s_k)|s_k|^{1+\gamma_3} \\ -c_3 s_k - \widehat{d}_k + \ddot{k}_d - \varsigma_k \dot{z}_k \end{pmatrix} \tag{40}$$

where the parameters satisfy the following:

$$c_1 = \frac{\pi \eta_3^{1/2}}{\gamma_3 T_3 \beta_3^{1/2}} \left(\frac{1}{2}\right)^{1-\frac{\gamma_3}{2}}, c_2 = \frac{\pi \beta_3^{1/2}}{\gamma_3 T_3 \eta_3^{1/2}} \left(\frac{1}{2}\right)^{1+\frac{\gamma_3}{2}},$$
$$c_3 > 0, \gamma_3 \in (0,1), \eta_3 > 0, \beta_3 > 0.$$

The stability property of the proposed attitude control law is demonstrated in the following theorem.

Theorem 3. *Consider the quadrotor UAV attitude subsystem (35) and (36), with the prescribed-time non-singular terminal sliding-mode surface (37) and the attitude control law (40). Suppose the following conditions hold:*

1. The desired attitude trajectories are bounded and differentiable;

2. The observer parameters satisfy $\alpha > 0,\ \beta > 0,\ 0 < \gamma < 1$*;*

3. The sliding mode surface parameters satisfy $\gamma_2 \in (0,1),\ \eta_2 > 0,\ \beta_2 > 0$*, and the controller parameters satisfy* $c_3 > 0,\ \gamma_3 \in (0,1),\ \eta_3 > 0,\ \beta_3 > 0$*.*

4. The prescribed time parameters satisfy $T_1 > 0,\ T_3 > 0$*.*

Then the attitude tracking error vector converges to a small neighborhood of the origin within the prescribed time, specifically: the sliding variable $s_k(t)$ *reaches a neighborhood of zero within time* T_3*, and consequently* $z_k(t)$ *is ultimately bounded with* $\mathcal{O}(\sqrt{\epsilon_k \varepsilon^2 / c_3})$ *for* $t \geq T_3$*, where* ε *is the disturbance observation bound from Theorem 1.*

Proof. Substituting (40) into (39) and using $\tilde{d}_k = d_k - \hat{d}_k$:

$$\dot{V}_k = s_k(-c_1 \text{sign}(s_k)|s_k|^{1-\gamma_3} - c_2 \text{sign}(s_k)|s_k|^{1+\gamma_3} - c_3 s_k + \tilde{d}_k) \tag{41}$$

Using Young's inequality on $s_k \tilde{d}_k$:

$$s_k \tilde{d}_k \leq \frac{s_k^2}{2\epsilon_k} + \frac{\epsilon_k \tilde{d}_k^2}{2}$$

Therefore,

$$\begin{aligned} \dot{V}_k &\leq -c_1|s_k|^{2-\gamma_3} - c_2|s_k|^{2+\gamma_3} - \left(c_3 - \tfrac{1}{2\epsilon_k}\right)s_k^2 + \tfrac{\epsilon_k \varepsilon^2}{2} \\ &\leq -c_1(2V_k)^{\frac{2-\gamma_3}{2}} - c_2(2V_k)^{\frac{2+\gamma_3}{2}} - \left(c_3 - \tfrac{1}{2\epsilon_k}\right)2V_k + \tfrac{\epsilon_k \varepsilon^2}{2}, \end{aligned} \tag{42}$$

where we used the observer bound $|\tilde{d}_k| \leq \varepsilon$ from Theorem 1 for sufficiently large t.

For the appropriate choice of ϵ_k such that $c_3 > \frac{1}{2\epsilon_k}$, the dominant terms yield the following:

$$\dot{V}_k \leq -\frac{\pi}{\gamma_3 T_3 \sqrt{\eta_3 \beta_3}}\left(\eta_3 V_k^{1-\frac{\gamma_3}{2}} + \beta_3 V_k^{1+\frac{\gamma_3}{2}}\right) + \frac{\epsilon_k \varepsilon^2}{2}. \tag{43}$$

According to Lemma 1, the system state vector reaches a small neighborhood of the sliding mode surface within a prescribed time T_3. Hence, the control system can converge to a small neighborhood of the origin within prescribed time $T = \max\{T_1, T_2, T_3\}$. □

Remark 8. *The ultimate bounds in both position and attitude loops can be made arbitrarily small by: (1) Increasing the observer gain* a_3 *to reduce* ε*; (2) Reducing the approximation parameter* δ_j *in the position controller; (3) Adjusting* ϵ_j *and* ϵ_k *to balance convergence rate and steady-state accuracy. In practice, these parameters are tuned to achieve desired tracking performance while maintaining control smoothness.*

5. Numerical Experiments

To verify the effectiveness of the proposed control method, simulations are carried out with designed parameters given in Table 1. Results show that the method in this paper can solve the trajectory tracking problem under composite disturbances within a prescribed time. As shown in Figure 2, the QUAV used in the simulation is able to track the desired trajectory by utilizing the control method proposed in this paper. Figure 3 shows that the position error converges to a small neighborhood of the origin within the user's prescribed time, and Figure 4 shows that the attitude error converges to a small neighborhood of the origin within the prescribed time as well. It can be seen that the proposed method

exhibits superior convergence accuracy when handling large initial deviations and strong composite disturbances, and that the convergence time constraints and robust stability are strictly satisfied. Figure 5 depicts the control inputs signals of position and altitude. The applied disturbances are matched (directly added to control channels via Equation (1)), time-varying (containing periodic sinusoidal components), and bounded with magnitude $|f_i(t)| \leq 0.2$ for all channels. The disturbance model $f_i = 0.1\sin(0.01t)\sin(0.1t) + 0.1\sin(i)$ captures both slow-varying environmental effects (wind gusts with 0.01 Hz modulation) and high-frequency oscillations (sensor noise at 0.1 Hz), representing realistic operational conditions for small quadrotors.

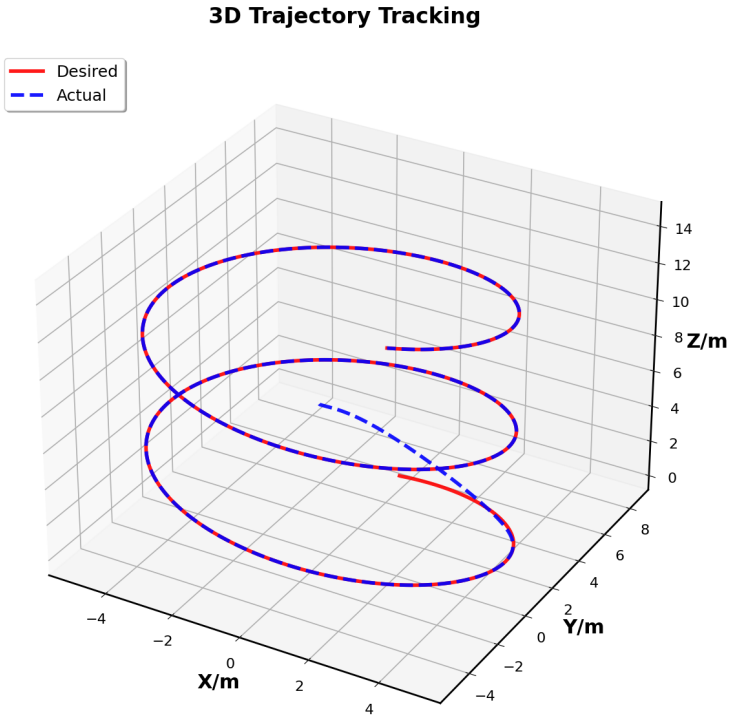


Figure 2. Trajectory tracking performance.

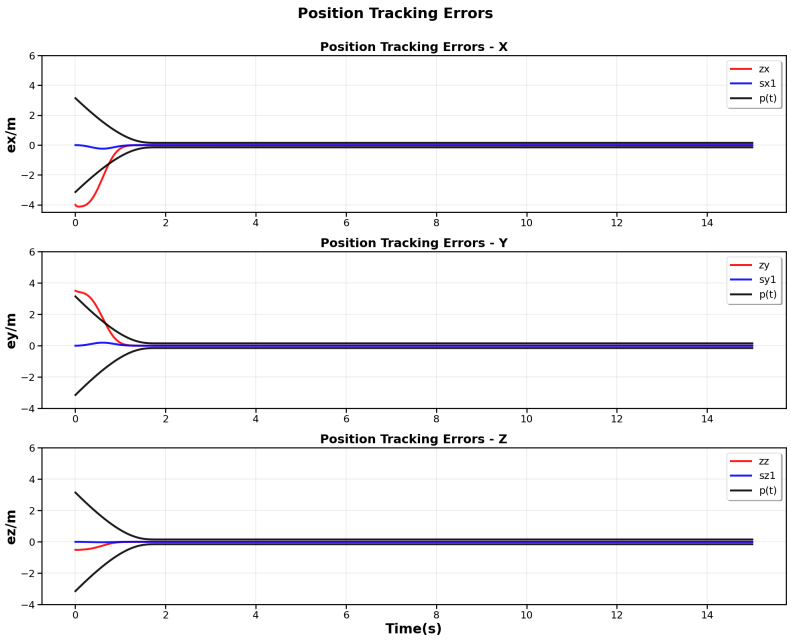


Figure 3. Prescribed-time convergence curve of the position error.

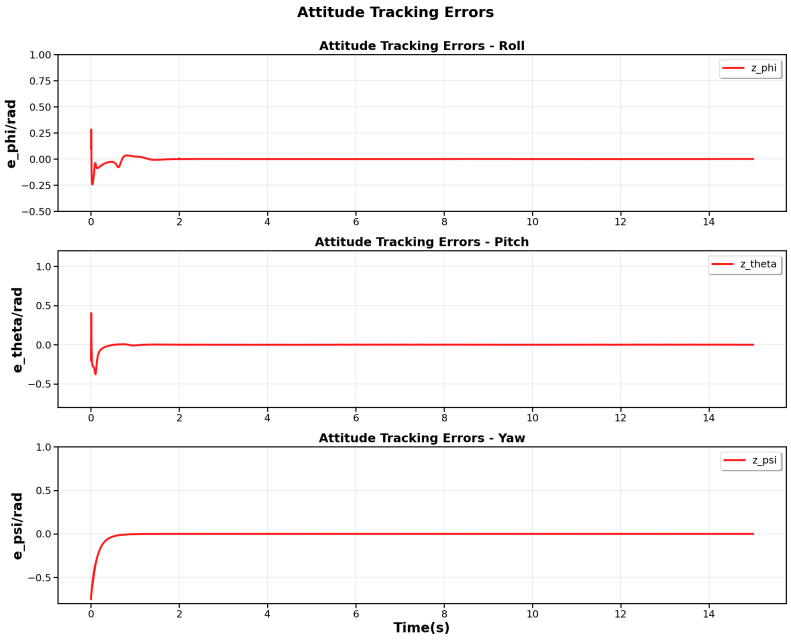


Figure 4. Prescribed-time convergence curve of the attitude error.

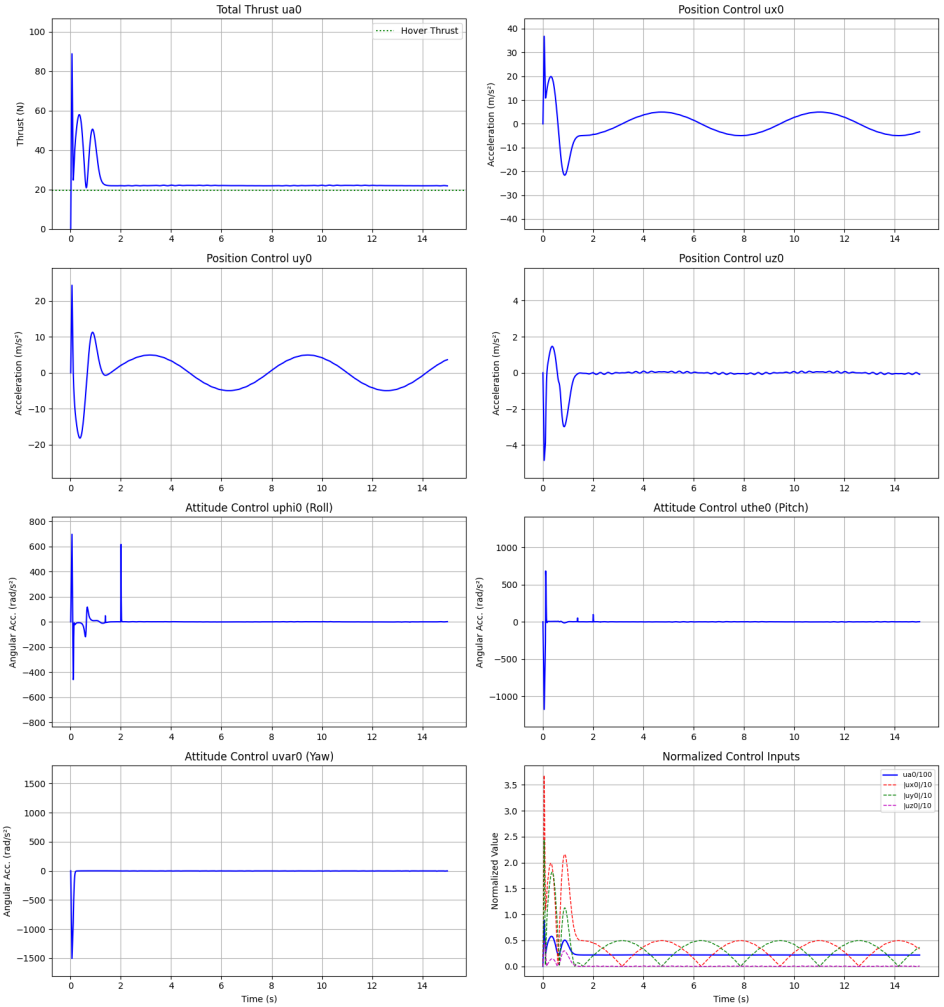


Figure 5. Control inputs performance.

Table 1. Simulation parameters.

Parameters	Value
Simulation Parameters	$m = 2,\ I_x = I_y = 1.24,\ I_z = 2.5,$ $K_x = K_y = K_z = K_\varphi = K_\theta = K_\psi = 0.01$
Disturbance	$f_i = 0.1\sin(0.01t)\sin(0.1t) + 0.1\sin(i)$ Type: Matched, time-varying, bounded Magnitude: $\lvert f_i(t)\rvert \le 0.2$ for all i
Reference signal	$x_d = 5\sin(t),\ y_d = 5\cos(t),\ z_d = t,\ \varphi_d = \pi/3$
Initial state	$x = -4,\ y = 8.5,\ z = -0.5,$ $\varphi = 0.1,\ \theta = -0.2,\ \psi = 0.3$
Prescribed time	$T_1 = 1,\ T_2 = 3,\ T_3 = 1$
PPC function parameters	$p_0 = 1.1,\ p_\infty = 0.15,\ \xi_0 = 0.001$
Observer parameters	$\gamma_1 = 0.5,\ \eta_1 = 0.1,\ \beta_1 = 0.5,\ a3 = 5$
Controller parameters	$\mu_{j1} = 30,\ \mu_{j2} = 35,\ \lambda_j = 50,\ \delta_j = 0.01,$ $\gamma_2 = 0.3,\ \eta_2 = 0.1,\ \beta_2 = 2,$ $\gamma_3 = 0.3,\ \eta_3 = 6,\ \beta_3 = 5,\ b_3 = 20$

5.1. Results Analysis

The actual position trajectories (x, y, z) closely follow their references (x_d, y_d, z_d) after the transient period, with steady-state errors remaining below the prescribed bounds. Similarly, the attitude angles (φ, θ, ψ) track their desired values with errors converging to small neighborhoods. These tracking accuracies are adequate for typical autonomous flight missions such as waypoint navigation and trajectory following.

This paper conducts a comparative analysis of four different methods (results are shown in Figures 6 and 7): PID control, terminal sliding mode control with extended state observer (TSMC-ESO), combination of prescribed performance control with extended state observer (PPC-ESO), and the method proposed in this paper (PTC-PPC-TSMC-ESO). It can be observed that the PID controller is insufficient to control the system in the presence of time-varying disturbances. The TSMC-ESO method exhibits suboptimal performance in the position loop control, but it can converge quickly in the attitude loop; however, the use of a sign function in the switching rate causes oscillations about the origin. The PPC-ESO method performs well in position loop control, but in the attitude loop, the convergence rate is unsatisfactory, and the states exhibit large fluctuations. Based on the comparison, the proposed method, which combines PPC, PTC, TSMC, and ESO, can significantly mitigate the shortcomings of the aforementioned methods, leading to substantial improvements in QUAV control under disturbances.

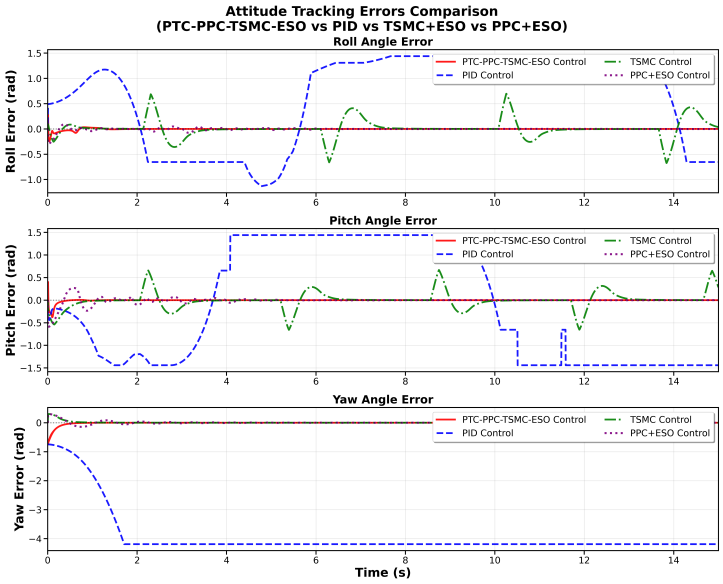


Figure 6. Position tracking error curves of the four methods.

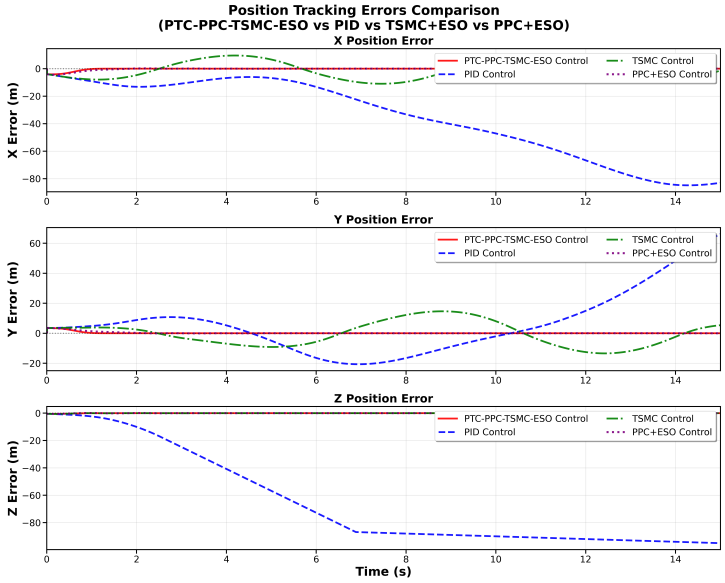


Figure 7. Attitude tracking error curves of the four methods.

5.2. Limitations and Future Directions

Despite the theoretical contributions and promising simulation results, several limitations of the proposed method should be acknowledged:

1. Need for systematic parameter tuning guidelines: The method involves the adjustment of over a dozen parameters across the observer and controllers. Although effective parameter sets have been demonstrated in simulation, systematic and efficient tuning strategies for different quadrotor platforms and mission profiles require further study and clear guidelines to facilitate practical deployment.

2. Higher real-time computational demand: The real-time computation of the disturbance observer and the derivatives of the barrier Lyapunov function imposes greater processing requirements compared to conventional PID controllers. Deployment on embedded hardware with sufficient computing power is necessary to maintain control rates above 100 Hz.

3. Dependence on model parameters: The control design relies on accurate model parameters such as moments of inertia I_x, I_y, I_z and drag coefficients K_i. While the disturbance observer enhances robustness to parametric uncertainties to some extent, control performance may still degrade when model errors are significant (e.g., exceeding $\pm 20\%$).

Future research directions:

- Experimental validation: Hardware-in-the-loop (HIL) testing and flight experiments on physical quadrotor platforms to validate control performance under real-world conditions, including sensor noise, actuator delays, and aerodynamic effects.
- Adaptive parameter tuning: Development of online learning algorithms (e.g., reinforcement learning or adaptive control) to automatically adjust controller gains based on flight conditions and disturbance characteristics.
- Extension to multi-UAV systems: Application of the proposed framework to cooperative control of heterogeneous multi-UAV formations with communication constraints, as motivated by recent work on resilient distributed control [9].
- Integration with perception systems: Combination of the proposed control with vision-based state estimation and obstacle avoidance for fully autonomous navigation in GPS-denied environments.

These directions aim to bridge the gap between theoretical advances and practical deployment, ultimately enabling prescribed-performance control in real-world UAV applications.

6. Conclusions

This article addresses the tracking control problem for QUAVs subject to unknown disturbances and large initial-state deviations by proposing a control method that integrates prescribed-performance control, prescribed-time control, a disturbance observer, and prescribed-time nonsingular sliding-mode control. The proposed method achieves prescribed-time satisfaction of performance constraints while ensuring exponential ultimate boundedness in the presence of persistent disturbances. Specifically, the position controller guarantees that tracking errors remain within prescribed bounds for all time, and the attitude controller ensures rapid convergence to a small neighborhood of the origin within prescribed time. A comparative analysis using simulations has been presented to demonstrate that the proposed method can not only rigorously achieve the prescribed-time convergence of position and attitude errors to small neighborhoods with the desired accuracy but also exhibit desirable performance under unknown disturbances and large initial deviations, significantly improving the trajectory-tracking accuracy and mission reliability of QUAVs.

Author Contributions: Conceptualization, T.X. and J.X.; methodology, T.X.; software, J.G.; validation, J.C., D.S. and D.L.; formal analysis, J.C.; resources, T.X.; writing—original draft preparation, T.X.; writing—review and editing, D.S.; visualization, J.G.; supervision, D.L.; project administration, D.S. All authors have read and agreed to the published version of the manuscript.

Funding: The paper is supported by the National Key Laboratory of Micro-Spacecraft Rapid Design and Intelligent Cluster [Funding Number: MS01240124] and National Natural Science Foundation of China [Grant Numbers: 62403032].

Institutional Review Board Statement: Not applicable.

Informed Consent Statement: Written informed consent has been obtained from the authors to publish this paper.

Data Availability Statement: The original contributions presented in this study are included in the article. Further inquiries can be directed to the corresponding author.

Conflicts of Interest: The authors declare no conflicts of interest.

References

1. Arafat, M.Y.; Alam, M.M.; Moh, S. Vision-Based Navigation Techniques for Unmanned Aerial Vehicles: Review and Challenges. *Drones* **2023**, *7*, 89. [CrossRef]
2. Mahony, R.; Kumar, V.; Corke, P. Multirotor aerial vehicles: Modeling, estimation, and control of quadrotor. *IEEE Robot. Autom. Mag.* **2012**, *19*, 20–32. [CrossRef]
3. Lee, T.; Leok, M.; McClamroch, N.H. Geometric tracking control of a quadrotor UAV on SE (3). In Proceedings of the 49th IEEE Conference on Decision and Control (CDC), Atlanta, GA, USA, 15–17 December 2010; IEEE: Atlanta, GA, USA, 2010; pp. 5420–5425.
4. He, M.; Chen, H.; Han, W.; Deng, C.; Duan, H. Development status and key technologies of cooperative control of bird-inspired UAV swarms. *Acta Aeronaut. Astronaut. Sin.* **2024**, *45*, 29946.
5. Raffo, G.V.; Ortega, M.G.; Rubio, F.R. An integral predictive/nonlinear H^{∞} control structure for a quadrotor helicopter. *Automatica* **2010**, *46*, 29–39. [CrossRef]
6. Eltayeb, A.; Rahmat, M.F.; Basri, M.A.M.; Eltoum, M.M.; Mahmoud, M.S. Integral adaptive sliding mode control for quadcopter UAV under variable payload and disturbance. *IEEE Access* **2022**, *10*, 94754–94764. [CrossRef]
7. Cui, Y.; Chen, J.; Lin, H.; Yang, X.; Meng, M.Q.H. Cooperative Multi-AAV Path Planning for Discovering and Tracking Multiple Radio-Tagged Targets. *IEEE Trans. Syst. Man Cybern. Syst.* **2025**, *55*, 2463–2475. [CrossRef]

8. Xu, G.; Xia, Y.; Zhai, D.H.; Lyu, W. Adaptive Finite-Time Attitude Tracking Control of Quadrotor Under Actuator Faults and External Disturbances with Guaranteed Performance. *Int. J. Adapt. Control Signal Process.* **2022**, *36*, 2662–2676. [CrossRef]
9. Liu, Y.; Dong, X.; Ren, Z.; Liu, J. Secure Formation Control for Resilient Multi-Agent Cyber-Physical Systems Under DoS Attacks and Faults. *Int. J. Robust Nonlinear Control* **2023**, *33*, 3607–3626. [CrossRef]
10. Polyakov, A. Nonlinear feedback design for fixed-time stabilization of linear control systems. *IEEE Trans. Autom. Control* **2011**, *57*, 2106–2110. [CrossRef]
11. Wang, T.; Ning, W.; Sun, Z.; Xia, Y. Prescribed-Time Trajectory Tracking Control for Quadrotor Without Velocity Measurement. *IEEE/ASME Trans. Mechatron.* **2025**, *30*, 5940–5951. [CrossRef]
12. Liu, H.; Huang, S.; Tu, H. Quadrotor sliding mode control based on predefined time. *J. Beijing Univ. Aeronaut. Astronaut.* **2022**, *50*, 1665–1674.
13. Yang, W. Development trend of navigation guidance and control technology for new generation aircraft. *Acta Aeronaut. Astronaut. Sin.* **2024**, *45*, 529720.
14. Wu, Y.; Hu, L.; Liu, L.; Zhang, Y.; Zhang, Y. Finite time prescribed performance control for stochastic systems with asymmetric error constraint and actuator faults. *Commun. Nonlinear Sci. Numer. Simul.* **2024**, *139*, 108290. [CrossRef]
15. Zhang, L.; Deng, C.; Che, W.W. Adaptive Backstepping Control for Nonlinear Interconnected Systems with Prespecified-Performance-Driven Output Triggering. *Automatica* **2023**, *154*, 111063. [CrossRef]
16. Zhao, Z.; Xiao, L.; Jiang, B.; Cao, D. Fast nonsingular terminal sliding mode trajectory tracking control of a quadrotor UAV based on extended state observers. *Control Decis.* **2022**, *37*, 2201–2210.
17. Wu, Y.; Zheng, B.; Li, H. Attitude controller for quadrotor via active disturbance rejection control and sliding mode control. *Electron. Opt. Control* **2022**, *29*, 93–98.
18. Labbadi, M.; Cherkaoui, M. Adaptive fractional-order nonsingular fast terminal sliding mode based robust tracking control of quadrotor UAV with Gaussian random disturbances and uncertainties. *IEEE Trans. Aerosp. Electron. Syst.* **2021**, *57*, 2265–2277. [CrossRef]
19. Ding, X.; Jin, X. Research progress of rotorcraft UAV interactive manipulation dynamic modeling. *Acta Aeronaut. Astronaut. Sin.* **2024**, *43*, 527388.
20. Liao, J.; Gao, X.; Yan, S.; Zhou, S.; Wang, D.; Kang, Y. Formation reconfiguration control of UAV swarm based on MPC-PIO. *J. Beijing Univ. Aeronaut. Astronaut.* **2022**, *50*, 1541–1550.
21. Cao, P.; Gan, Y.; Dai, X. Finite-time disturbance observer for robotic manipulators. *Sensors* **2019**, *19*, 1943. [CrossRef]
22. Wang, J.; Zhao, L.; Yu, L. Adaptive terminal sliding mode control for magnetic levitation systems with enhanced disturbance compensation. *IEEE Trans. Ind. Electron.* **2020**, *68*, 756–766. [CrossRef]
23. Liu, W.; Chen, M.; Shi, P. Fixed-Time Disturbance Observer-Based Control for Quadcopter Suspension Transportation System. *IEEE Trans. Circuits Syst. I Regul. Pap.* **2022**, *69*, 4632–4642. [CrossRef]
24. Jia, T.; Yan, H.; Zhang, H.; Li, H.; Zhang, Y. Adaptive anti-disturbance performance guaranteed formation tracking control for quadrotor UAVs via aperiodic signal updating. *IEEE Trans. Syst. Man Cybern. Syst.* **2024**, *54*, 5212–5223. [CrossRef]
25. Bouabdallah, S.; Siegwart, R. Backstepping and sliding-mode techniques applied to an indoor micro quadrotor. In Proceedings of the 2005 IEEE International Conference on Robotics and Automation, Barcelona, Spain, 18–22 April 2005; IEEE: Barcelona, Spain, 2005; pp. 2247–2252.
26. Yao, Q.; Li, Q.; Huang, M.; Jahanshahi, H. Predefined-time trajectory tracking control of free-flying space manipulator subject to uncertainties and disturbances. *Robot. Auton. Syst.* **2024**, *177*, 104699. [CrossRef]
27. Liu, K.; Wang, R.; Zheng, S.; Dong, S.; Sun, G. Fixed-time disturbance observer-based robust fault-tolerant tracking control for uncertain quadrotor UAV subject to input delay. *Nonlinear Dyn.* **2022**, *107*, 2363–2390. [CrossRef]
28. Liu, C. Research on Adaptive Tracking Control of a Climbing Robot for Wooden Columns. Ph.D. Thesis, Shandong Jianzhu University, Jinan, China, 2020.
29. Yin, C.; Wu, Q.; Yang, S.; Zhou, C. Guaranteed performance predefined time Control for manipulator with arbitrary initial state. *Modul. Mach. Tool Autom. Manuf. Tech.* **2025**, *2025*, 103–108, 113.

Disclaimer/Publisher's Note: The statements, opinions and data contained in all publications are solely those of the individual author(s) and contributor(s) and not of MDPI and/or the editor(s). MDPI and/or the editor(s) disclaim responsibility for any injury to people or property resulting from any ideas, methods, instructions or products referred to in the content.